COMPONENT PART NOTICE

THIS PAPER IS A COMPONENT PART OF THE FOLLOWING COMPILATION REPORT:

TITLE: Transonic and Supersonic Phenomean in Turbomachines: Proceedings of the

Propulsion and Energetics (68th)(B) Specialists' Meeting Held in Munich,

Germany on 10-12 September 1986.

TO ORDER THE COMPLETE COMPILATION REPORT, USE __AD-A182 996__ .

THE COMPONENT PART IS PROVIDED HERE TO ALLOW USERS ACCESS TO INDIVIDUALLY
AUTHORED SECTIONS OF PROCEEDING, ANNALS, SYMPOSIA, ETC. HOWEVER, THE COMPONENT
SHOULD BE CONSIDERED WITHIN THE CONTEXT OF THE OVERALL COMPILATION REPORT AND
NOT AS A STAND-ALONE TECHNICAL REPORT.

THE FOLLOWING COMPONENT PART NUMBERS COMPRISE THE COMPILATION REPORT:

AD#: __AD-P005 506 thru AD-P005 523.__   AD#: _____

AD#: _____   AD#: _____

AD#: _____   AD#: _____

DTIC
ELECTE
AUG 1 7 1987
S   D
A

DTIC FORM 463
MAR 85

OPI: DTIC-TID

WAKE AND SHOCK INTERACTIONS IN A TRANSONIC TURBINE STAGE

by

D.L.Schultz and A.B.Johnson
Dept. of Engineering Sciences
Oxford University
Oxford OX1 3PJ, UK

D.A.Ashworth and M.J.Rigby
Rolls Royce
Derby, UK

and

J.E.LaGraff
Syracuse University
N.Y., USA

Abstract

The strong trailing-edge shock waves from the nozzle guide vanes of transonic turbine stages can give rise to interactions with the downstream rotor which are significantly more severe than is the case with lower pressure ratio stages. It is therefore important to study such effects in detail both from the point of view of stage power output and more importantly from that of heat transfer rates. A study has been made of a transonic rotor profile in a static cascade in which the effect of shock wave interaction is simulated by means of an array of bars rotating at the correct speed and spacing upstream of the stationary rotor blades. Detailed heat transfer rate measurements made with rapid response gauges enable the wake and shock phenomena to be separated.

Nomenclature

C_2 = NGV exit velocity, relative bar velocity

C_t = Tangential (or true) chord

k = Thermal conductivity (W/mK)

$\dot{q}$ = Heat transfer rate (W/m²)

M = Isentropic Mach Number (based on local static pressure and inlet total pressure)

Nu = Nusselt Number

Re = Reynolds Number (based on inlet total conditions, isentropic exit Mach Number and tangential chord)

s = Blade surface perimeter

t = Time

T = Temperature (K)

Tu = Turbulence level = $u'/\bar{U}$

u' = Fluctuating velocity (m/s)

U = Velocity (m/s)

V = Rotor relative velocity, cascade inlet velocity

x = Surface distance from the leading edge stagnation point

y_b = Distance in the pitch-wise direction from the spanwise datum position

β = Gas angle (measured from the axial direction)

Subscripts

∞ = Freestream

o = Total

1,2 = Inlet, Outlet

meas = Measuring point

h,m,t = Hub, mean, tip (or tangential in chord definition)

rel = Relative bar condition

Introduction

The effects of unsteady flows caused by rotor blade/NGV interactions and the disturbance to the potential flow due to rotor blade motion are arousing increasing interest as attempts are made by turbine designers to improve their predictions of performance. Previous work by Doorly[1-3] and Dunn[4-10] has shown the significant effect of NGV-rotor interaction on heat transfer rates associated with the effect of the turbulent NGV wake on the rotor boundary layer as the blade passes through the wake. Doorly's studies have identified the fluid dynamic phenomena associated with the interaction employing a stationary linear cascade and an array of bars rotated off-axis upstream of the blades in such a way as to generate a set of wakes which pass over an instrumented stationary blade. Dunn's studies, on the other hand, involved a complete rotor behind an NGV ring. An extensive study of unsteady secondary flow vortices in a turbine rotor stage has been made by Binder et al.[11-13]. Laser two-focus velocimetry was used to track the distortion and migration of the NGV passage vortex as it passed through the rotor blade ring. Simultaneous measurements of mean velocity and turbulence level were made. It was found that the turbulence level arising from this vortex was raised considerably by the cutting action of the rotor blades and this effect was ascribed by Binder et al. to the break-up of the vortex itself. The experiments were carried out in a steady flow turbine rig so that the long sampling times required for accurate L2F measurements were readily attainable. Hodson[13] has also investigated the blade-wake interaction measuring unsteady blade pressures on a large-scale rotating rig in a manner similar to that at UTRC where Dring and his colleagues[14-15] have studied blade boundary layers using a rotor axis fixed hot wire anemometer.

The work reported in the present study has been carried out in a linear cascade of the blades of a transonic stage where the NGV exit Mach Number is generally higher than that used by Doorly or Dunn and in which the strong recompression shocks in the wake have a more important effect on the boundary layer and hence on the heat transfer rates. The rotor profile is the same as that currently fitted to the MIT transient blowdown facility described by Epstein et al.[16] so that direct comparisons will be possible between the two different approaches.

Experimental Apparatus

The measurements were carried out in the isentropic light piston cascade described by Schultz et al.[17], in which a short duration (~ 0.5 sec.) flow is produced at the correct full-scale engine Reynolds and blade exit Mach Numbers and at the correctly scaled gas/wall temperature ratio. The simulation employed, i.e. stationary rotor and moving wakes has advantages in terms of simplicity over the fully rotating experiment in so far as Schlieren techniques may be employed to locate shock waves and boundary layer separations (induced, it will be seen, by the incident shock wave). It must be emphasised, however, that the following effects are not simulated:

1. Temperature gradients in the wake due either to a film cooled NGV or the heat transfer to the vane as a whole.

2. The differential effects of buoyancy forces on the cooled wake and the mainstream flow.

3. Distortion of the NGV passage flow by the rotor blockage.

4. The influence of unsteady secondary flows over both the rotor root and the tip region.

The simulation is, in effect, valid only for mid-blade height flows but is believed to be valuable nevertheless in that it enables the relevant fluid dynamic phenomena to be isolated and studied in some detail. The arrangement of the linear cascade, the rotating disc and stranded steel cables is illustrated in Fig. 1(a). A more complete description is given by Ashworth et al.[18] and it suffices here to record that the aerodynamic design of the prototype cold air turbine in which a 61 blade rotor spins at 9004 RPM behind an NGV ring of 36 vanes is correctly simulated by having a disc carrying 16 radial bars (stranded cable) and a turbine scaling factor cascade/cold air turbine of 1.3247. The NGV trailing edge diameter was 1.2192 mm and the nearest suitable cable diameter of 1.6151 mm was chosen for convenience. The plane of the array of the bars was located 14.333 mm upstream of the cascade blade leading edge line. Experiments reported by Doorly[1-3] have shown that a wake velocity profile similar to that from an NGV can be produced by a circular cylinder of diameter equal to that of the vane trailing

edge. The cascads has a span of 50 mm at hleda inlet and 56.095 mm at exit with the expansion on one eide only ae iliustrated in Fig. 1(a). A turhulenoe grid 208 mm upetream of the cascade provides a level of $u'/\bar{U}$ of approximately 3%. Upetream and downstream etatio and total proseures were measured routinely to estahlieh the correot cascada operating oonditions and are rsported in more detail hy Ashworth et al.[19]. The operating conditions at the nominai engine design point are given halow.

The heat transfer gaugae used in this etudy are oonventional thin flim eurfaoe resistance thermometere widely used for the daterimination of heat tranefer rate in short duretion faoiiities[19]. Data from 22 euoh geugee wera etored in a digital traneient recorder eampling up to 16 ohannais at 500 kHz for each ohannel or wera input direotly to tha A/D oonvertar at a elower rata of 400 Hz for soma of the 64 avaiiahla A/D ohannele when time avar_ge data oniy were required, aleo uned for meas-remente suoh ae inlet and exit etatio preesuree. The looations of theee heat tranefer gauges on the hiade era shown in Fig. 2(a) and givan in terme of the eurfaoe length 'x' to perimeter 'e' from the etagnation point. A more dstailed etudy of the reaotion of the euotion eurfaoa houndary iayar to hoth freeetream turhuienoa and the wake-paesing phenomene ie aleo reportad heiow. For thie etudy another hiada wae instrumented with thin film gaugee whioh were only 4 mm long as oompared to 10 mm for the pravious taets, and were mors oloesly epaoed around the profila. as ehown in Fig. 2(h). The model pointe in Fig. 2(h) ara those referred to in Fig. 6. Surfaoe praseuree ware meaeured in e time-averaged manner ueing Seneym semioonductor transduoers type LX-1620D operating in a differantial mode ee raported in more detaii hy Ashworth et al.[19]. Baseline experimentel resulte have heen reported hy Ashworth et el. hut for olerity some of thie data is referred to in the preeent paper. The velocity triangle for tha stsady nominai design cese ie shown in Fig. i(h) whioh inoludes the effeot of the reduoed NGV exit waks velooity C_2' on the rotor inlet angle β_1.

Experimental Results

Mean Heat Transfer Without Wake Interaction

A comparieon of haseline deta with no rotor/waka intaraction ie given in Fig. 3(a) for the two casae of low (< 0.8%) freeetream turhulenoa end with a turbulenoa level of approximately 3%. It will ha seen that ths turhulsnce genereted hy the har grid ia euffioient to hring ths region of boundery layar transition forwerd from ahout 60% x/e on the preesura eurfeoe and 50% x/e on tha euotion surfaoe to 10% and 20% respeotively. All of this data wae takan et tha nominal dwsign oasoada opereting oonditione:

$$T_{total} = 432 \text{ K}$$
$$M_{exit} = 1.18$$

(hased on isentropio inlet total and pitohwiee averaged exit stetio preeaurae)

$$Re = 0.919 \times 10^6$$
$$\beta_1 = 58.06°.$$

The oiroled numhers refar to heat tranefer gaugee identified in Fig. 2(e). The heat transfar reta is praeented in terms of a non-dimaneional Nuseelt Numher, defined ee:

$$Nu = \frac{q_{meas}}{(T_o - T_{msas})} \frac{C_t}{k}$$

Instantaneous and Mean Heat Transfer with Wake Interaction

Tha heat tranafer rete to the hlada with tha additionel effeot of wake intaraction is illustrated in Figs. 3(b) and 3(o) for both oases of affaotively zero freeetream turbulenoe and ~ 3% $u'/\bar{U}$. From Fig. 3(c) it will he eeen that there ie an overell inoreaae in haat transfer rata over both the preasure and suotion aurfecaa. Tha praesura aurfaca hsat tranefar ia enhanoed ovar praotioally tha whola langth although tha dominant effeot ie oheervad for valuee of x/a < 70%. On the pressure aurfaoa the affeot of waka interaotion persiets to ahout x/a = 30%. Examplea of inatantaneous heat transfar ratae are inaet in the Figure and a more axtansiva 'atlas' of reaults ia givan in Aahworth at al.[19]. The heat tranafar rataa with wake interaotion and with effeotivsly zaro freastream turbulanoa era ahown in Fig. 3(h). As expeoted thera ia a marked inoraaae in tha lavel of heat tranefer rata ovar almoet the entire preeeure

and euotioe eurfeoee.   Examplee of instantaneoue values of heat tranefer rate ere ineet and theee eleo illustrate the increeee over tbe undieturbed oeee.

Mean Effects of Inlet Incidence Angle on Heat Transfer Rate and Pressure Distribution

Ae ie illuetrated in Fig. 1(b) the paeeage of the reduced velooity wake through the rotor hlading givee riee to e time varying obange of inoidenoe angle. Although thie ohange ie eeeooieted with the blade-wake ieteraotion thero ie neverthelese e time-averaged effeot wbiob leade to quite marked varietione, partioularly on tbe euotioe eurfaoe heet tranefer rete and preeeure dietrihutioe. Coneidering firet tbe heet transfer rete, Fig. 4(e), illuetretee the more prolonged region of laminar heat transfer rate aeeooieted with e deoreased ieoidenoe of -10° from deeign velue of 58.06°. Studiee et an inoreased inoideeoe of 63.06° were cerried out for off-deeign performanoe purpoeee only and eltbough reported here for pefereeoe ere eot e pert of the overall wake-blade interaotion experimeete. The uneteady inoideeoe effeote oeueed hy tbe wake velooity defioit ere eot oorreotly eimuleted hy meaeuremeete made ie tbe eteady etate but it ie probahle that tbe eeture of the traneient obangee, et leaet eeer the leeding edge, ere ie liee with thoee ehowe. Similer remarke epply to tbe effeot of e deoreased ieoidenoe oe Maob Number dietrihutioe around tbe hlede, Fig. 4(h), the overall reeult being e reduction of Maoh Number, i.e. unloeding of tbe orown of the euotion eurfeoe, x/e < 40%.

Measurement of the Unsteady Disturbance at Inlet

Ie order to uederetand the unsteedy pheeomeoe oeueed hy tbe her-paseing epparetue, e eketoh of the expeoted inlet dieturhanoee ie the eimuletioe and tbe engiee ie givee in Fig. 5(e). The velooity triangles ere matohed by eetting tbe oorreot her velocity and matohing tbe oeeoede ielet velooity to tbe rotor reletive velooity. The ietermitteet perturbetione to tbe ielet flow oeueed by tbe eimulatioo ere ebowe for the high freeetrsam turhuleooe ceee ie Fig. 5(b) ie terms of hot-wire output from tbe probe mounted ie the freeetream ielet plane et mid-paseage, eod eurfeoe etagnetioe poiet measuremeete of preseure and heet tranefer rete. Botb theee reeulte and tbe deteiled measuremeete on tbe suotion eurfeoe are preeeeted from teete ueing tbe ber-paseing epperetue deeoribed ebove witb juet 2 here fitted, ee oppoeed to the 16 here neoeeeery to model the oorreot blede paseieg frequeeoy of the oold-eir turbiee deeige. Thie enehlee individuel her-paseing eveete to he seperated in time, einoe it ie diffioult to tell whetber evente were merging togetber from tbe 16 bar experimento elone. Thie dete ia normalised witb reepoot to 2 oyolee the ber-peeeieg eveet, eo tbat it ie poeeibie to relete ieformation from different rune io terme of oyole freotion. Tho eigeele ehow e baokground turbuleet level extending over ebout 60% of the oyole oberaoterieed by e eimiler type of eignel to thet ohteined witb eo roteting bere. All tbree eigeele heve e periodic oompooent et bar-peseing frequeeoy witb two ohereoterietio perte:

(i) Over ebout 6% of tbe oyole repid ohangee in level of tbe order of 5 to 10 µe riee and feil timee are observed. The preeeure eigeel variee by +/- 25% and the beet transfer rate by epproximately +/- 50%. This dieturbenoe ia ettributed to ehook wevee generated as tbe her eueepe past tbe oeecade. By examieetion of Sobliereo photographe of tbie flow, examplea of whioh ere given io Fig. 7, tbe neture of the NGV eimuleted ehook atruoture oan be determined. Cleerly two ehooke ere aeeooieted witb ooe ber-paeeing event, the bow end reoompreeeion ehooke tbat would be expected et tbe ber reletive Maoh Number in steady flow. The eeparetioe time between these ehooke ie approximately 75µs, marked as At$_e$ io Fig. 5(h), and ie eeee to oorreepond to the time ieterval hetween tbe eherp felle ie level to the adjeoeet eharp peak.

(ii) Following theee repidly obanging eveete, a eeoond leee marked change in level aseooieted with the wake ie elao vieihle over about 10% of the oyole, marked ee tbe "wake" regioe io Fig. 5(h).

Time-Resolved Heat Transfer Rate Measurements on the Suction Surface

The eeture of the reaotion of otherwiee laminar boundary layere to both e higber level of isotropic freeetream turbuleeoe, and to tbe intermitteet dieturbanoee oeueed by tbe wake and ehook/boundary leyer ietereotione wee ievestigeted ie more deteil using tbe instrumeeted auction aurfeoe shown io Fig. 2(b), and tbeee reeulte ere preeeeted in Fig. 6.

(o) Noturai Transitios of the Suotios Surfaos Bousdsry Laysr

Wide bandwidth hsst transfsr signals ohtsised from tbo ourfaoe tbis film gauges olsarly illustrsts tbs important diffsresoos betwssn ths low and higb frssstream turhulssos oasss as sbown in ths higb frequssoy traoso of Fig. 6(a). Thsre is a oonstant spacing of 5 mm bstwoan tbo tbin film gauge rssults ohown, starting with gsuge 3 at as x/s vsiua of 0.12 through to gauge 15 at x/o = 0.65. Ths low turbuiesou osse (Run 5723) remaiss quist (iamisar) throughout ths sstire measuring rangs of ths transisst data (to x/o = 0.65). Ths surfaoe bsst transfor for ths bigb frssstrsam turbuissoe oass, wbils starting somewhat highsr than ths iaminar osss, beoomss isorsosingly dominsted by sharp trancisnt svsnts (oossistent witb tbs thsory of turhulsst spot dsvsiopmsst, growtb, and g:adual msrgsr as proposed by Emmoss[16] and vsrifisd by many others (s.g. Sohubausr and Kishasoff[11]). Thsss spots, whioh raise ths hsst transfsr ooeffioisst instantansousiy to high turbulsst lsvcio, oostisus to grow and msrgs ustil finsliy ths Nusosit Numbsr oignals beooms inoreasingly obarsotsrieed by tbs "stsady" turbuisnt lsvsis. It is olsarly sses that hy tho x/s = 0.65 stetion ths flow is at ths turbuisst isvsl mors than half of tbs time hut drops prsoissly to ths usdisturbed laminar values bstwssn the turbulsst evsnts. Is othsr tests oonduoted at 1.5 x Rs dssign, the boundsry laysr was fully turbulsst st this looatios.

Ths physioal prooss of turbulsst spot hreakdown to turbuisnos oan bs sses in Fig. 6(a). Ths growth and rearward oosvsotion of individual turhulsst spots is olearly sssn as thsy movs aiong the blads surfsos. Ths spot signals grow is hsight and width as tbs opots oovsr mors of saoh suooseding thin fiim gauge and sbift in time downstrsam. This brsakdown prooss is quantified is mors detaii is Ashworth[11] whsre istsrmittssoy lsvsls are estimated from ths digital time rsoordn and spot oosvsotios ratss srs sstimated from oross-oorrslation analysis of sdjoining tbis film sigsals.

(b) Detaiisd Waks and Shook Intsrsotios Effeots

It is possiblu to analyss ths reactios of ths biads houndsry isysr to ths wake and shook perturbatiosa with 2 bars rotatisg hy isvsstigatijn of ths sequsscs of time-resoived Nusssit Numbsr plots givss is Fig. 6(h),(o) and (d). The higb freestrsam turbuissoe oass witb wakes and sbooks prsssst (Fig. 6(h)) is markedly diffarent to the saturally transitionai boundary laysr (Fig. 6(s)) ovsr tbs first 35% of tbe surfaoa, witb simiiar rspid rises and falls is Nusssit Numbsr to the psrturbationo svidsst is Fig. 5. This sbook relsted svsst ocours or the sariy suotion surfaos dus to a shook/boundary layer istersotios starting at gsuge 9, oloss to ths crows of the suotios surfaoe. Examination cf ths Sohlisren photographs (Fig. 7) isdioatos that ths shooks first intsraot with the boundsry laysr ssar to gsuge 9, ths reflsotios poist moving towards ths lsading-edgs ac tbs bar movss is ths same direotios. This ie visihls on the early gaugss on Fig. 6(h), ocourring firet on gsuge 9 tbss moving graduaily through gsugss 7 and 5 and fisslly showing on gauge 3. The rapid drop is surfaoe Musselt Numbsr is sttrihuted to an unatsady assparstion and ths riss to a turbulsst rs-attaohmest both oaused by the shook houndary laysr intsraotion. Ths sffeot of ths wake is not olsariy disosrnabie in Fig. 6(h) and to sid in idsntifioatios of this tbs bars wsre rotated at a lowsr apsed suoh tbat tbs bar relativs Maoh Numbsr was suheonio. The resuita of this are shown as Fig. 6(u) with a muoh mors oisarly idsstifiabis snhanoemest is hsat transfsr dus to tbis waks. This sxtsnds to tbs latsr gaugss of the surfaoe oausing ths boundary layer to be fuily turbulent ovsr ths sxtsnt of tha wake. Is Fig. 6(d) the baokground turbulsnoa wss reduoed to lsss than 0.8% and the periodio disturbanoss due to the bar-passing svests are more olsarly evidsst. The sarly suotion surfaos has shook-related phssomsna sxtsnding well isto the oyole period with apparsst osoillations is Nusssit Numbsr soving with tbe shook. Also spparent from Fig. 6(d) ie ths istsrmittest nature of the turbulsnoe induoed in ths boundary layer hy the waks and shook intsraotion, as tbs boundary layer oisarly returns to its usdisturbed laminar value betwees the periodio svests. The hsat transfsr snhanoemest dus to ths waks is oisarly svidsst along the whois surfaos.

In summary, it appsirs that ths stats of ths turbine boundary laysr seems to be oontrolled hy the levsi of freestream turhulsnos sxoept during ths time for whioh ths shook and wake aotuaily pass through ths oasoada passage.

Schlieren Photographs of the Wake and Shock Interaction

In Fig. 7 Schlieren photographs showing four passages of the cascade (marked A to D) are presented for five instants in the bar-passing cycle. This reflected Schlieren technique gives changes in tone corresponding to the integrated effects of density gradient across the span of the cascade, so that events running normal to the tunnel sidewall show up most clearly. With no bars present the general mid-tone appearance varies most at the trailing-edge shocks with some effects due to the high accelerations near to the leading-edges. The photographs in Fig. 7 are from the 2 bar tests, as the pictures become somewhat confusing in the high-frequency wake-passing case. The position of the bar is shown corresponding to time 1, 26 μs before the bar reaches its datum position at 90° to the tunnel sidewall. The tip of the bar enters and leaves the cascade when the bar radial line is inclined at +/- 45° to its datum position, but over the range of photographs shown this angle varies from -3° to 17° thus amounting to 11% of the cycle between bar-passing events. The shock and wake events are evident in all of these photographs so is detailed here for each of the times in Fig. 7:

1. The bow shock is visible in passage C as a thin horizontal line just touching the crown of the suction surface. The curved end of this shock is due to refraction from the leading-edge of the upper blade of this passage, so the shock was chopped here as the bar swept by, vertically downwards from the point of view of these photographs. Some weak shock activity is evident in passage D, as will be discussed below. Passage C contains some reflected shock activity associated with the bar recompression shock. The wake can be seen as a mottled region in passage A covering more than half of the passage.

2. 71μs later the bow shock has passed the lower blade leading-edge of passage C and is now being refracted from this point. The recompression shock is now in passage C, with its distorted shape due to reflection effects. The wake is now visible in both passages A and B.

3. After another 65μs the bow shock has nearly left the lower passage (D), with a quite strong reflected shock visible as a series of arcs, due to the three-dimensional nature of the shock as will be described below. The recompression shock is close to the leading-edge of the upper blade of passage D, also reflected across the passage. The wake is steadily encroaching in to the two upper passages (A and B).

4. The reflection of the recompression shock in passage C is still evident, and the refraction of the same shock in the lower passage is now overlapping with the reflection of the bow shock, which now also is reflecting again from the pressure surface. The wake is now starting to appear in passage C.

5. A short time (30μs) later the shock activity has almost cleared passage C, save for some weak secondary reflections of the recompression shock still evident, surprisingly reflecting again off the suction surface. It is assumed that these weaker shock interactions would not have much effect on the boundary layer state, but could cause some of the oscillations in heat transfer noticeable only in the cases where M_{rel} (the bar relative Mach Number corresponding to U_{rel}) is transonic.

Predictions of the Wake and Shock Positions

2-Dimensional Wake Predictions

For the five times corresponding to the Schlieren photographs shown in Fig. 7, predictions of the wake position were calculated, the results of which are shown in Fig. 8. The wake itself is almost 2-dimensional in form, varying mainly in height across the span due to the 3-dimensional bar geometry, so that only a 2-dimensional calculation is necessary. The procedure follows that described in Doorly[*], now fully automated and allowing for the spreading of the wake by using a width proportional to the square-root of the distance from the bar along the line of U_{rel} with the constant of proportionality derived from a database of wake measurements. The prediction procedure is as follows:

(i) A prediction of the flowfield velocity is made, in this case using the Denton scheme[24] and stored by the program.

(ii) U_{rel} is calculated (assumed constant across the span), the center-line of the undistorted wake is calculated from the specified bar position and the width added.

(iii) The wake is shifted back in time so that the bar will return to its correct position following the marching process of the prediction routine.

(iv) From this initial position elements of the wake are convected by small time steps using the local velocity interpolated from the prediction until the bar reaches the specified location. The differential velocities in the flowfield cause distortion of the wake along its length and across its width as it is accelerated through the passage.

This simple scheme, which could be incorporated in the blade design process, agrees well with the positions of the wake on the Schlieren photographs, so that the fraction of time that the heat transfer rate to the surface is effected by the wake could be calculated and included in the intermittency term of a prediction. It also demonstrates that to the level of our measuring ability second-order effects such as the "negative jet" effect do not significantly effect the wake position, as referred to in Doorly[21], and that the assumption that this flow unsteadiness may be superimposed on the steady flowfield is a valid approximation.

Quasi-3-Dimensional Shock Prediction

Although it was possible to model the wake in 2-dimensional terms, the shock structure associated with the transonic nature of the bar (as M_{rel} varies from 1.06 at the hub to 1.25 at the tip) is not strictly 2-dimensional, as has been seen in the Schlieren photographs (Fig. 7). An attempt was made to predict the positions of the bow and recompression shocks due to the bar in order to allow trajectory rate calculations to be made relating to the heat transfer measurements, and to aid in understanding phenomena observed in the Schlieren photographs. An example of such a prediction is presented as Fig. 9. The prediction is based on the assumption that for a small element of the bar the flow is 2-dimensional with respect to the plane containing U_{rel} and normal to the bar axis, a quasi-3-dimensional approach described in detail in Ashworth[22]. As U_{rel} varies in both magnitude and direction, so does the associated shock structure, and unlike the wake, this variation should be accounted for. The method of prediction was computerised as follows:

(i) For assumed constant inlet conditions and a specified position of the bar M_{rel} is calculated and its direction determined.

(ii) The equation of the bow shock in the 2-dimensional plane described above is derived from M_{rel} using the method described in Shapiro[24], shock properties and turning angles obtained by curve-fit equations where necessary over a range of Mach Number from 1.0 to 1.5.

(iii) The recompression shock is assumed to be straight and inclined at the Mach angle $(\sin^{-1} 1/M_{rel})$ to the direction of M_{rel} with a virtual origin two diameters downstream of the bar.

(iv) The shocks are chopped and refracted if they are downstream of the blade axial leading-edge point, with allowance made for regeneration of the shock as it moves away from this point.

(v) Finally the points of intersection with the blade suction surface are calculated, and the shocks are simply reflected from an origin mid-way between the two intersection points.

Comparison with the Schlieren photographs is encouraging, the position shown in Fig. 9 corresponding to time 2 in Fig. 7., and it is hoped that information from this simplified model will prove useful as an aid to understanding the complex shock movements in turbine passages, in spite of the many simplifying assumptions made in this prediction (such as allowing for no variation of the freestream velocity).

Conclusions

It has been established during the course of this study that the Isentropic Light Piston Tunnel facility combined with the wide bandwidth/high sampling rate heat transfer instrumentation has proved capable of tracking very rapidly progressing unsteady events in a transonic boundary layer. Operating

under a simulated unsteady gas turbine rotor environment, sensitive detection and precision tracking of transient shock, wake and boundary layer transitional events was accomplished.

A second major outcome of this study was the observation that the strong unsteady interaction of a double shock and a simulated NGV wake with the rotor boundary layer did not have any measurable "long-term" effects apart from the strong excursion in heat transfer associated with the actual passing of the shocks and wake. The heat transfer fluctuation levels were essentially unchanged far removed from the disturbance (in time) and nearly identical at the rearmost measuring point except for a turbulent patch associated with the shock/wake event itself.

The interaction of the shocks and wake with the rotor establishes in more detail the earlier observation of Ashworth et al.[10] and Doorly and Oldfield[1] of strong changes in local heat transfer coefficient. The tracking of the interaction over the surface could be followed with some precision with the time resolution of the instrumentation used.

Predictions of the positions of both the wake and shock structures caused by the bar are most encouraging, as they are based on simplified models easily incorporated in the design process, unlike many other methods which are to unwieldy for turbine designers to use. They both are based on superimposing the unsteady structures on existing steady-state information, and as such agree well with measured data.

Acknowledgements

References

1. Doorly, D. .. and Oldfield, M. L. G., "Simulation of Wake Passing in a Stationary Turbine Rotor Cascade", J. Eng. for Gas Turbines and Power, ASME, Vol. 107, pp. 998-1006, 1985.

2. Doorly, D. J. and Oldfield, M. L. G., "Simulation of the Effects of Shock Wave Passing on a Turbine Rotor Blade", ASME Paper No. 85-GT-112, 1985.

3. Doorly, D. J., Oldfield, M. L. G. and Scrivener, C. T. J., "Wake Passing in a Turbine Rotor Cascade", AGARD CP-390, pp. 7.1-7.18, 6th May, 1985.

4. Dunn, M. G. and Hause, A., "Measurement of Heat Flux and Pressure in a Turbine Stage", ASME J. Eng. for Power, Vol. 104, pp. 215 223, 1982.

5. Dunn, M. G., Lukis, G., Urso, M., Haimenz, R. J., Orazuiak, R. and Key, N. J., "Instrumentation for Gas Turbine Research in Short Duration Facilities", Aerospace Congress, Long Beach, CA, Paper No. 841504, 15th - 18th October, 1984.

6. Dunn, M. G., Rae, W. J. and Holt, J. L., "Measurement and Analysis of Heat-Flux Data in a Turbine Stage", Parts I and II, J. Eng. for Power, Vol. 106, No. 1, January, 1984.

7. Dunn, M. G., Martin, H. L. and Stanek, M. J., "Heat Flux and Pressure Measurements and Comparison with Prediction for a Low Aspect Ratio Turbine Stage", ASME Paper No. 86-GT-79.

8. Dunn, M. G., "Heat Flux Measurements for a Rotor of a Full-Stage Turbine: Part I - Time-Averaged Results", ASME Paper No. 86-GT-77.

9. Dunn, M. G., George, M. K., Rae, M. J., Woodward, S. H., Moller, J. C. and Seymour, P. J., "Heat-Flux Measurements for the Rotor of a Full-Stage Turbine: Part II - Description of Analysis Technique and Typical Time-Resolved Measurements", ASME Paper No. 86-GT-78.

10. Dunn, M. G., "Experimental Measurements of Heat-Flux Distributions in a Turbine Stage with Upstream Disturbances", Advanced Earth-to-Orbit Propulsion Technology Conference, Huntsville, Alabama, 13th - 15th May, 1986.

11. Binder, A., Foerster, W., "Turbulence Production due to Secondary Vortex Cutting in a Turbine Rotor", ASME Paper No. 85-GT-13.

12. Binder, A., Foerster, W., Mach, K. and Rogge, H., "Unsteady Flow Interaction Caused by Stator Secondary Vortices in a Turbine Rotor", ASME Paper No. 86-GT-302.

13. Hodson, H. P., "An Inviscid Blade-to-Blade Prediction of Wake Generated Unsteady Flows", ASME Paper No. 84-GT-189, 1984.

14. Dring, R. P. and Joelyn, H. D., "The Relative Eddy in Axial Turbine Rotor Passages", ASME Paper No. 83-GT-22, 1983.

15. Dring, R. P., Joelyn, H. D., Hardin, L. W. and Wagner, J. H., "Turbine Rotor-Stator Interaction", ASME J. Eng. for Power, Vol. 104, pp. 729-742, 1982.

16. Epstein, A. H., Guenette, G. R. and Norton, R. J. G., "The MIT Blowdown Turbine Facility", ASME Paper No. 84-GT-116, 1984.

17. Schultz, D. L., Jones, T. V., Oldfield, M. L. G. and Daniels, L. C., "A New Transient Cascade Facility for the Measurement of Heat Transfer Rates", AGARD CP-229, 1977.

18. Ashworth, D. A., LaGraff, J. E., Schultz, D. L. and Griodrod, K. J., "Unsteady Aerodynamic and Heat Transfer Processes in a Transonic Turbine Stage", ASME Paper No. 85-GT-128, 1985.

19. Schultz, D. L. and Jones, T. V., "Heat Transfer Measurements in Short Duration Hypersonic Facilities", AGARDOGRAPH No. 165, 1973.

20. Emmons, H. W., "The Laminar-Turbulent Transition in a Boundary Layer - Part I", J. Aero. Sci., Vol. 18, No. 7, July, 1951.

21. Schubauer, G. B. and Klebanoff, P. S., "Contributions on the Mechanics of Boundary Layer Transition", NACA Report 1289, 1956.

22. Ashworth, D. A., LaGraff, J. E., and Schultz, D. L., "Unsteady Interaction Effects on a Transitional Turbine Blade Boundary Layer", Paper to be presented at the Joint ASME/JSME Gas Turbine Conference, March, 1987.

23. Doorly, D. J., "A Study of the Effect of Wake Passing on Turbine Blades", D.Phil. Thesis, University of Oxford, 1983.

24. Denton, J. D., "An Improved Time-Marching Method for Turbomachinery Flow Calculation", ASME J. Eng. for Power, Vol. 105, pp. 514-520, 1983.

25. Ashworth, D. A., "Unsteady Wake and Shock Interactions on a Transonic Turbine Blade", D.Phil. Thesis, University of Oxford, 1986.

26. Shapiro, A. S., "The Dynamics and Thermodynamics of Compressible Fluid Flow", Ronald Press, Vol. 2, pp. 884-886, 1954.
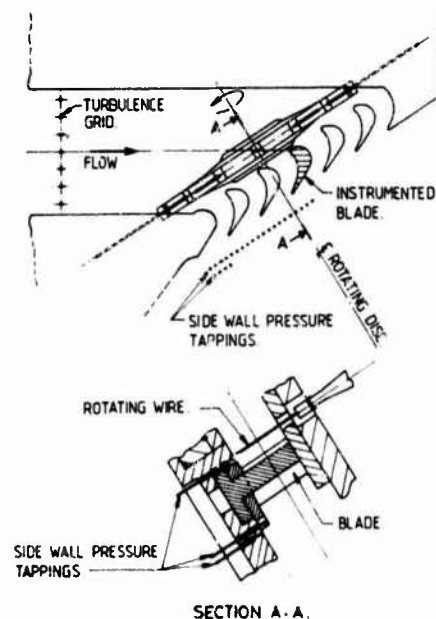
Fig. 1(a) Arrangement of the rotating bar wake generator and cascade.
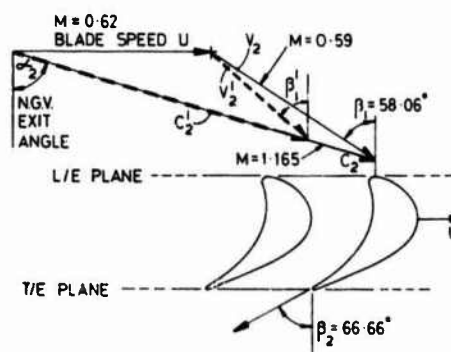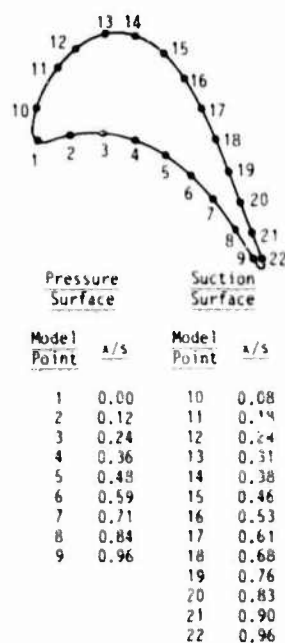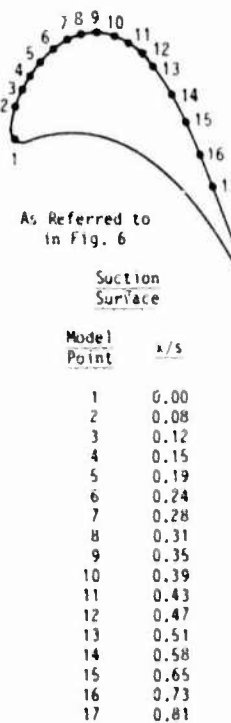
Fig. 1(b) Velocity triangles at inlet for the steady nominal design case at mid-span, showing the reduced incidence caused by the deficit in the wake.

Pressure Surface		Suction Surface		Suction Surface	
Model Point	x/s	Model Point	x/s	Model Point	x/s
1	0.00	10	0.08	1	0.00
2	0.12	11	0.19	2	0.08
3	0.24	12	0.24	3	0.12
4	0.36	13	0.31	4	0.15
5	0.48	14	0.38	5	0.19
6	0.59	15	0.46	6	0.24
7	0.71	16	0.53	7	0.28
8	0.84	17	0.61	8	0.31
9	0.96	18	0.68	9	0.35
		19	0.76	10	0.39
		20	0.83	11	0.43
		21	0.90	12	0.47
		22	0.96	13	0.51
				14	0.58
				15	0.65
				16	0.73
				17	0.81

(a)   (b)

Fig. 2(a) Co-ordinates of the original heat transfer gauges on the blade profile.

Fig. 2(b) Co-ordinates of the heat transfer gauges for the detailed suction surface study, referred to in Fig. 6.
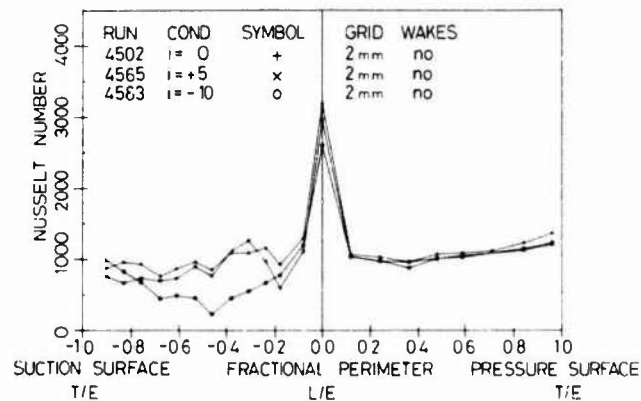
Fig. 4(a) Effect of incidence variation on mean heat transfer rate at the nominal design case
(M₂ = 1.18, Re = 0.919E6) with no wake and shock interaction.
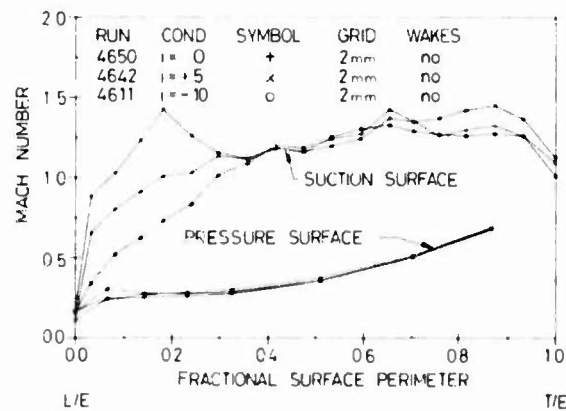

Fig. 4(b) Effect of incidence variation on mean surface isentropic Mach Number at the nominal
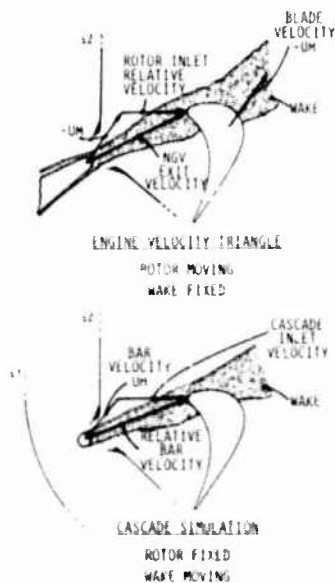design case (M₂ = 1.18, Re = 0.919E6).

Fig. 5(a) Illustration of the comparative
velocity triangles for the engine
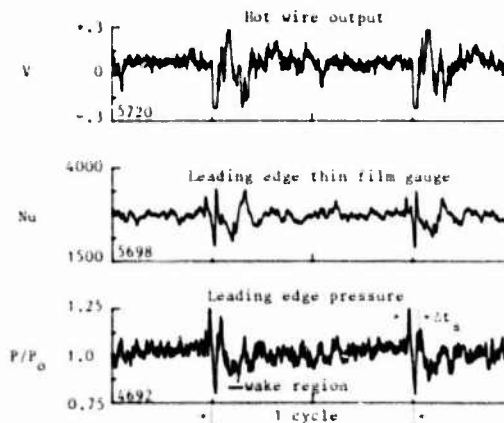and cascade simulation of the NGV/
rotor interaction.

Fig. 5(b) Measurements of the unsteady distur-
bance at inlet by a hot-wire in the
freestream and heat transfer and
pressure measurements at the stag-
nation point.

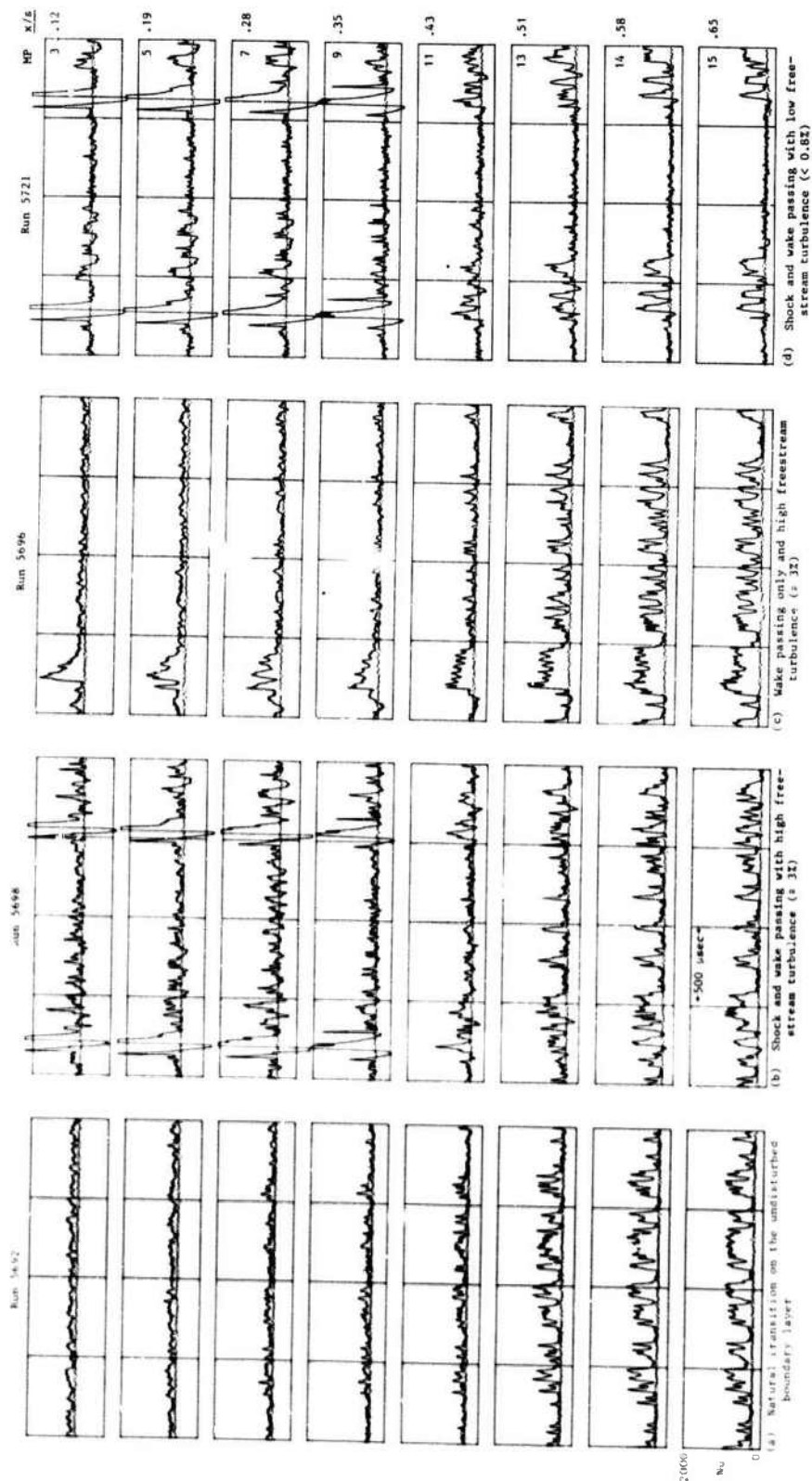
Fig. 6 Detailed time-resolved heat transfer rate measurements to the blade suction surface. The dotted lines are the baseline undisturbed results for the low freestream turbulence case (< 1%, Run 5723).
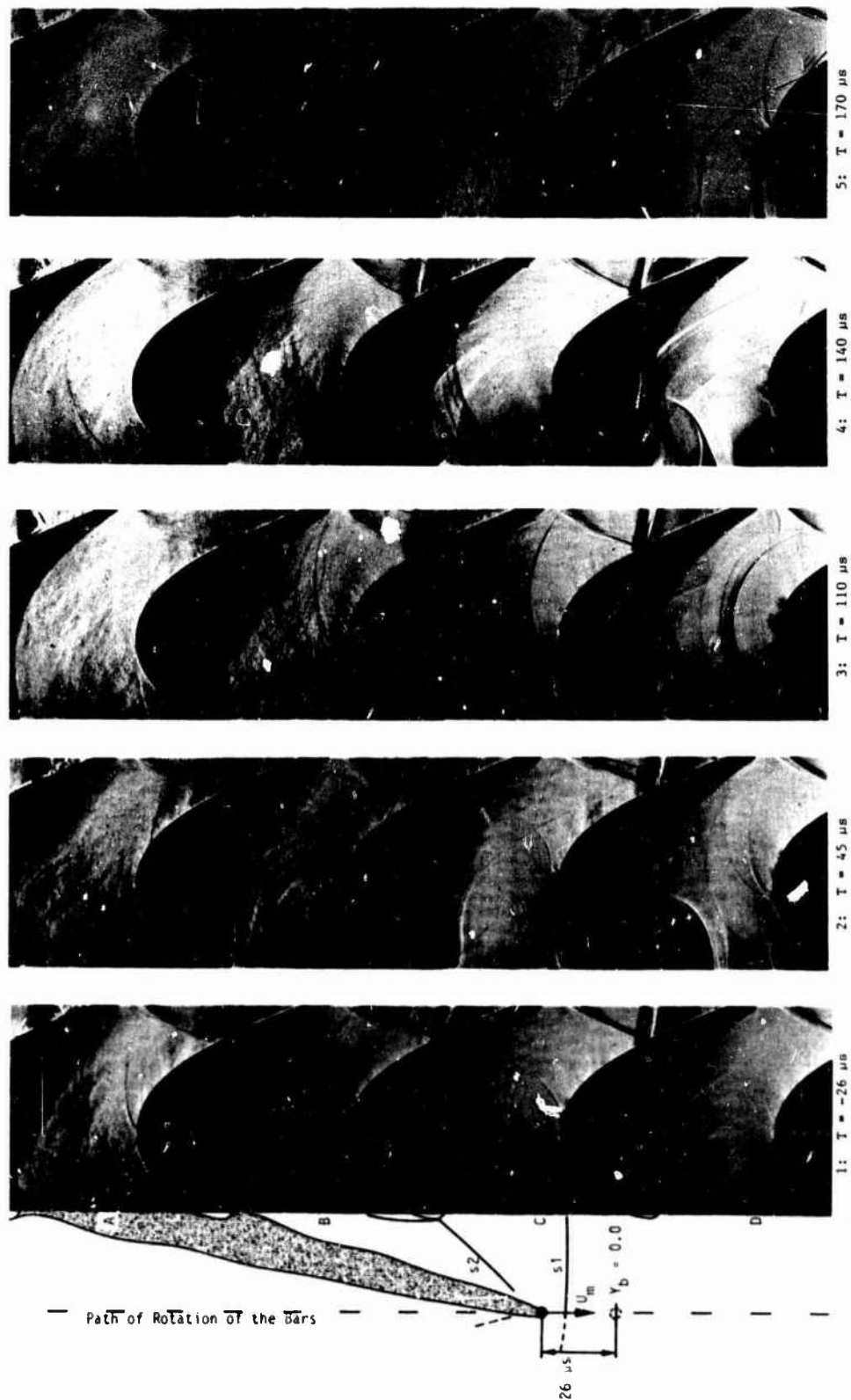
3-14

Fig. 7 Schlieren photographs of the cascade for different times in the bar-passing cycle. The position of the bar corresponding to time 1, the left-hand photograph, is illustrated with a sketch of the expected wake and shock positions (not visible in the photographs due to the limits of the Schlieren window).

Instrumented
Blade

Cascade
Pitch
= 34.3 mm

Axial
Chord
= 34.82 mm

A

B

C

0

U_m

D

Y_b +

0

1: T = -26 μs
Y_b = -7 mm

2: T = 45 μs
Y_b = 12 mm

3: T = 110 μs
Y_b = 29 mm

4: T = 140 μs
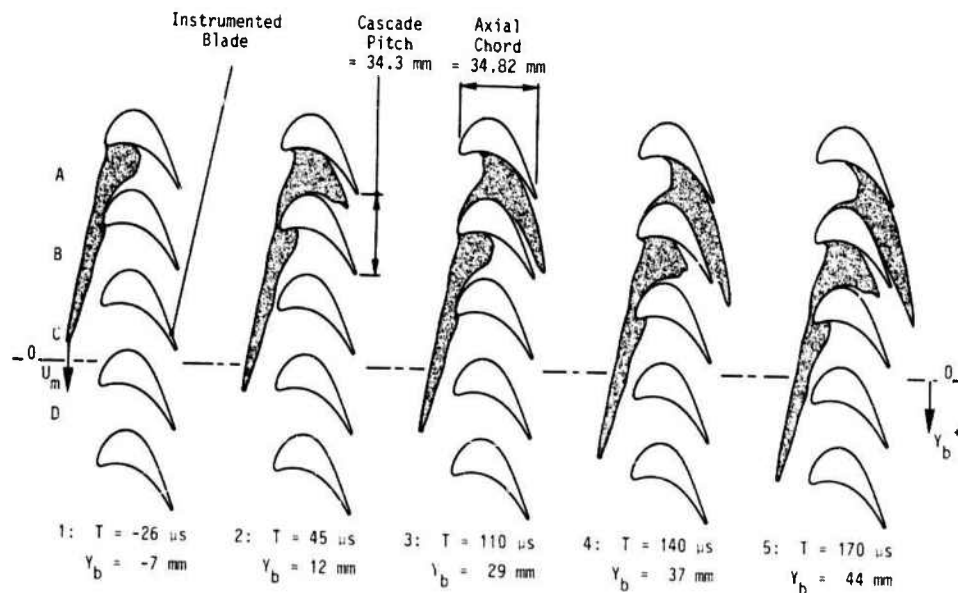Y_b = 37 mm

5: T = 170 μs
Y_b = 44 mm

Fig. 8 Predicted wake positions at times corresponding to the Schlieren photographs in Fig. 7.
The two lines for each time are the leading and trailing edges of the highly turbulent
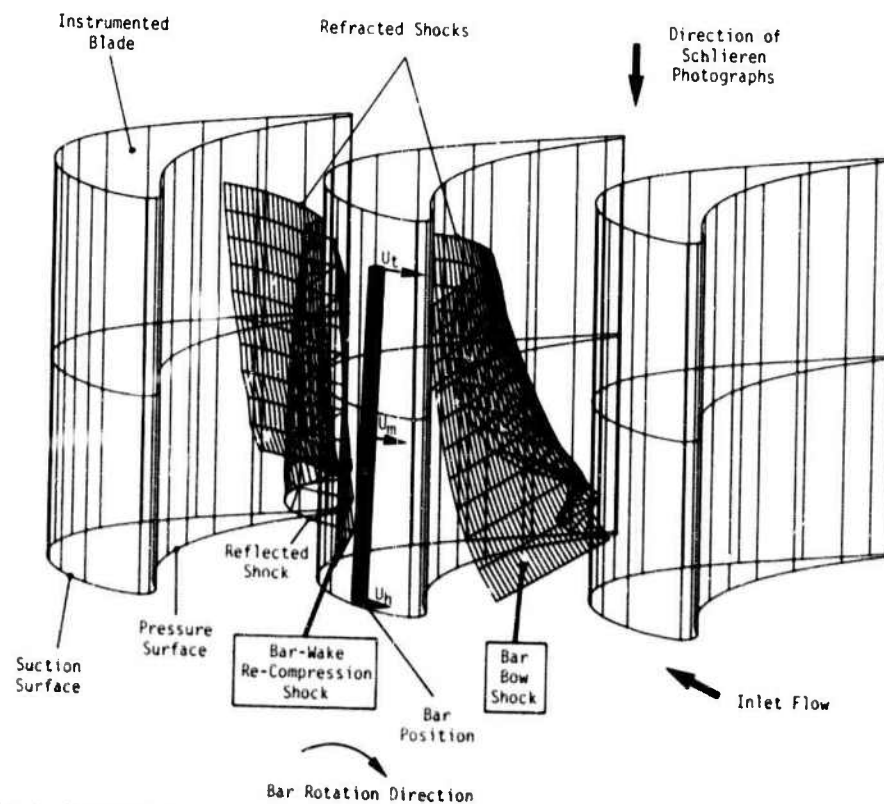wake region.

Instrumented
Blade

Refracted Shocks

Direction of
Schlieren
Photographs

U_t

U_m

U_h

Reflected
Shock

Bar-Wake
Re-Compression
Shock

Bar
Position

Bar
Bow
Shock

Inlet Flow

Suction
Surface

Pressure
Surface

Bar Rotation Direction

Fig. 9 Predicted shock position correeponding to time 2 of Fig. 7, with the bar inclined at
- 2° to its datum position. Only the half of the shocks downstream of the bar are
shown for clarity. The refraction and reflection of both shocks can be seen, with the
re-compression shock more 2-dimensional in form than the detached bow shock, due to
stand-off distance variation with bar relative Mach Number. Both shocks are weaker
towards the hub due to the lower Mach Number there, with the bow shock strength less
than the re-compression shock strength at each radius.

DISCUSSION

P.Ramette, Fr

The wake is induced, in your experiment, by a bar with a diameter corresponding to the nozzle trailing-edge section, which is symmetrical, while the nozzle wake is non-symmetrical. Consequently, you do not have the same gradients. How representative of a nozzle wake effect is your experiment?

Author's Reply

The work reported here is the follow-up of work carried out on a different profile, with a lower relative bar Mach Number, as reported by Doorly[27]. Prior to these tests, static tests were carried out by inserting a bar in a cascade with NGV's mounted in the same test section. It was therefore possible to traverse both bar and nozzle wakes and it was noted that the bar wake was quite representative of the NGV wakes. The larger momentum deficit corresponding to the suction side boundary layer that one would expect to contribute to the asymmetry did not appear to be significant and we assumed the same to be true for our cascade. It is worth noting that the weaker shock in the experiments reported by Doorly[1-3] only caused a boundary separation once the shock passed the leading edge of the blade. It is very interesting that quite different results can be obtained from similar experiments with only a few parameters altered, the most important of which is the shock strength.

[27]Doorly, D.J., "A Study of the Effect of Wake Passing on Turbine Blades", D.Phil Thesis, University of Oxford, 1983.